Rapid Communications

Variation of zero-energy density of states of a *d*-wave superconductor in a rotating in-plane magnetic field: Effect of nonmagnetic impurities

Yuuki Hashitani,[1] Kenta K. Tanaka,[1] Hiroto Adachi,[1,2] and Masanori Ichioka[1,2]
[1]*Department of Physics, Okayama University, Okayama 700-8530, Japan*
[2]*Research Institute for Interdisciplinary Science, Okayama University, Okayama 700-8530, Japan*

(Received 29 July 2019; revised manuscript received 18 November 2019; accepted 22 January 2020; published 7 February 2020)

Oscillation of zero-energy density of states under the rotation of an in-plane magnetic field is used to identify node positions of the superconducting gap. Based on Eilenberger theory that can capture the vortex core contribution appropriately, we quantitatively study the effects of nonmagnetic impurity scattering on the oscillation in a $d_{x^2-y^2}$-wave superconductor, as a function of the magnetic field and the scattering rate in the Born and the unitary limits. We find that the sign of the oscillation can be changed by the impurity scattering at low fields, indicating that impurity effect is an important factor in the analysis of angle-resolved specific heat measurements.

DOI: 10.1103/PhysRevB.101.060501

In unconventional superconductors with pairing mechanism other than the conventional electron-phonon interaction, anisotropic pairing symmetries such as p, d, and f waves are realized rather than the isotropic s wave. Therefore, in order to understand the pairing mechanism of unconventional superconductivity, we have to identify the pairing symmetry including the node positions of the pairing function. For the purpose, angle-resolved specific heat measurement is one of the powerful experimental methods. There, the position of nodes or gap minimum is examined from the small oscillation of low temperature specific heats under the rotation of applied magnetic field's orientation. These experiments have been already done in various superconductors such as heavy fermion superconductors [1–3], topological superconductors [4–6], and Fe-based superconductors [7–10].

In the theoretical studies of the angle-resolved specific heat, we consider the zero-energy density of states (DOS) $N(E=0)$, which is proportional to the specific heat at low temperature T. In the vortex state, $N(E=0)$ is sometimes estimated by the calculation of the Doppler shift [11,12]. While the idea of Doppler shift provides intuitive explanation for the oscillation of $N(E=0)$ under the rotation of magnetic fields, the calculation does not include the contribution of the vortex core since the amplitude of the pair potential is assumed to be uniform in the real space. Therefore, for an exact estimate of the oscillation of $N(E=0)$, we need self-consistent calculation of the vortex structure by Eilenberger theory in the vortex lattice state [13,14]. The DOS $N(E)$ is used to evaluate also the T dependence in the oscillation of the specific heat [15–17]. Eilenberger theory is derived under the assumption $\Delta_0/E_{\rm F} \ll 1$ for the superconducting gap Δ_0 and Fermi energy $E_{\rm F}$. In heavy fermion superconductors, $\Delta_0/E_{\rm F}$ becomes larger but still smaller than 1. Thus, experimental data of angle-resolved specific heat in these superconductors was well explained by Eilenberger theory [1–3]. Since many previous theoretical studies were done only in the clean limit, we need systematic studies to clarify whether the impurity effect seriously changes the oscillation of $N(E=0)$ or not. Experimentally, the impurity effect was reported in FeSe [10].

The purpose of this work is to clarify the nonmagnetic impurity effect on the oscillation of $N(E=0)$ under the rotation of in-plane magnetic fields in a fundamental case of $d_{x^2-y^2}$-wave pairing with line nodes [3,11–13,15–17]. We evaluate the oscillation of $N(E=0)$ by quantitative calculation of self-consistent Eilenberger theory in the vortex lattice state [13–15,18–23] and study the dependence on the magnetic field B and the scattering rate $1/\tau_0$ both in the Born and the unitary limits.

For simplicity, supposing an energy dispersion $\varepsilon = \hbar^2(k_a^2+k_b^2)/2m - t_c\cos(k_c c_c)$ with small t_c, we consider a quasi-two-dimensional rippled cylindrical Fermi surface with a Fermi velocity $\boldsymbol{v}_{\rm F} = (v_a, v_b, v_c) \propto (\cos\theta, \sin\theta, \Gamma^{-1}\sin(k_c c_c))$ at a Fermi wave number $\boldsymbol{k} = (k_a, k_b, k_c) \sim (k_{\rm F}\cos\theta, k_{\rm F}\sin\theta, k_c)$ in the crystal coordinate. We set the anisotropy ratio Γ of the coherence length as $\Gamma = 2$ in our calculation. This is a simple Fermi surface model for $CeCoIn_5$ [3,15]. The pair potential is $\Delta(\boldsymbol{r})\varphi_d(\theta)$ with the pairing function $\varphi_d(\theta) = \sqrt{2}(k_a^2-k_b^2)/k_{\rm F}^2$ for the $d_{x^2-y^2}$-wave pairing. $\boldsymbol{r}$ is the center-of-mass coordinate of the pair. Magnetic fields $\boldsymbol{B}$ are applied along the orientation of angle ϕ from a axis within the ab plane. In the calculation of the vortex structure, we use the vortex coordinate $(x, y, z) = (b\cos\phi - a\sin\phi, c, a\cos\phi + b\sin\phi)$, so that $\boldsymbol{B} = (0, 0, B)$ in the vortex coordinate. The vector potential is given by $\boldsymbol{A}(\boldsymbol{r}) = \frac{1}{2}\boldsymbol{B}\times\boldsymbol{r} + \boldsymbol{a}(\boldsymbol{r})$ in the symmetric gauge. We assume that the unit cell of the vortex lattice is triangular lattice rescaled by Γ, as in the inset of Fig. 1.

We calculate the spatial structure of vortices in the vortex lattice state by self-consistent Eilenberger theory [13–15,18–21], including self-energy from nonmagnetic s-wave impurity scatterings [22–29]. This method appropriately captures

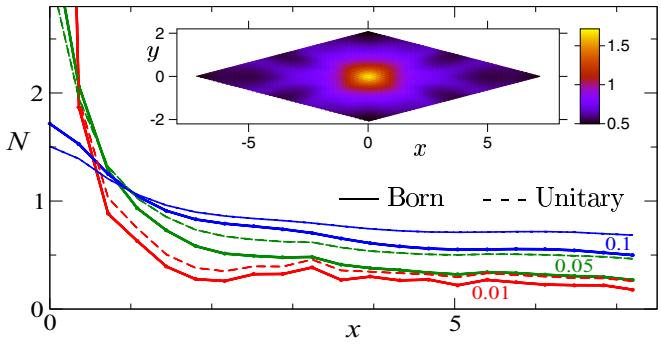

FIG. 1. Zero-energy local DOS $N(E=0,\boldsymbol{r})$ as a function of radius x from the vortex center along the x axis for $1/\tau_0 = 0.01, 0.05$, and 0.1 in the Born limit (solid lines) and the unitary limit (dashed lines). $B=2$, and $\phi = 0^\circ$. Inset shows density plot of $N(E=0,\boldsymbol{r})$ within a unit cell of the vortex lattice for $1/\tau_0 = 0.1$ in the Born limit. Vortex center is located at $(x, y) = (0, 0)$.

contributions of vortex core and intervortex interaction. In previous studies [13,14], vortex states under the rotation of in-plane magnetic field were calculated in the clean limit. We introduce contributions of the impurity scatterings in the calculation method. To obtain quasiclassical Green's functions $g(\mathrm{i}\omega_n,\boldsymbol{k},\boldsymbol{r})$, $f(\mathrm{i}\omega_n,\boldsymbol{k},\boldsymbol{r})$, and $f^\dagger(\mathrm{i}\omega_n,\boldsymbol{k},\boldsymbol{r})$, we solve Riccati equations obtained from Eilenberger equations [30–33]

$$\{\omega_n + G + \boldsymbol{v}\cdot(\nabla + \mathrm{i}\boldsymbol{A})\}f = (\Delta\varphi_d + F)g,$$
$$\{\omega_n + G - \boldsymbol{v}\cdot(\nabla - \mathrm{i}\boldsymbol{A})\}f^\dagger = (\Delta^*\varphi_d^* + F^\dagger)g, \qquad (1)$$

where $g = (1 - ff^\dagger)^{1/2}$, $\boldsymbol{v} = \boldsymbol{v}_\mathrm{F}/v_\mathrm{F0}$ with $v_\mathrm{F0} = \langle \boldsymbol{v}_\mathrm{F}^2\rangle_{\boldsymbol{k}}^{1/2}$. $\langle\cdots\rangle_{\boldsymbol{k}}$ indicates the Fermi surface average. In our calculations,

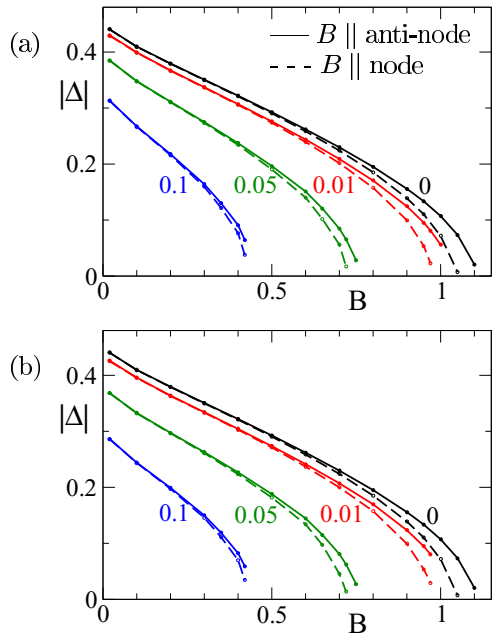

FIG. 2. Spatial average of the amplitude $|\Delta(\boldsymbol{r})|$ as a function of the magnetic field B for $1/\tau_0 = 0$, 0.01, 0.05, and 0.1 in (a) the Born limit and (b) the unitary limit. Solid (dashed) lines are for the case when $\boldsymbol{B}$ ∥ antinode ($\boldsymbol{B}$ ∥ node).

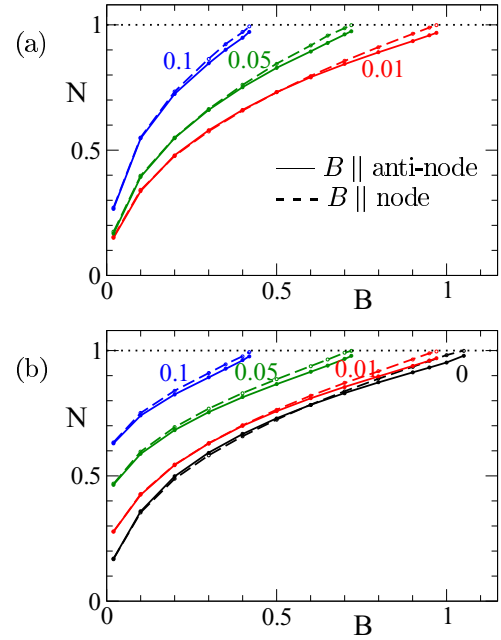

FIG. 3. Zero-energy DOS $N(E=0)/N_0$ as a function of the magnetic field B for $1/\tau_0 = 0.01$, 0.05, and 0.1 in (a) the Born limit and (b) the unitary limit. In (b), we also present lines for the clean limit $1/\tau_0 = 0$. Solid (dashed) lines are for N_antinode (N_node) when $\boldsymbol{B}$ ∥ antinode ($\boldsymbol{B}$ ∥ node).

length, temperature, and magnetic field are, respectively, measured in units of ξ_0, T_c, and B_0. Here, $\xi_0 = \hbar v_\mathrm{F0}/2\pi k_\mathrm{B}T_\mathrm{c}$ and $B_0 = \phi_0/2\pi\xi_0^2$ with the flux quantum ϕ_0. T_c is superconducting transition temperature in the clean limit at $B=0$. The energy E, pair potential Δ, and Matsubara frequency ω_n are in units of $\pi k_\mathrm{B}T_\mathrm{c}$. Within the t-matrix approximation [22–29], self-energies $G(\mathrm{i}\omega_n,\boldsymbol{r})$, $F(\mathrm{i}\omega_n,\boldsymbol{r})$, and $F^\dagger(\mathrm{i}\omega_n,\boldsymbol{r})$ in Eq. (1) are given by

$$G = \frac{1}{\tau}\langle g\rangle_{\boldsymbol{k}},\ F = \frac{1}{\tau}\langle f\rangle_{\boldsymbol{k}},\ F^\dagger = \frac{1}{\tau}\langle f^\dagger\rangle_{\boldsymbol{k}}, \qquad (2)$$

$$\frac{1}{\tau} = \frac{1/\tau_0}{\cos^2\delta_0 + (\langle g\rangle_{\boldsymbol{k}}^2 + \langle f\rangle_{\boldsymbol{k}}\langle f^\dagger\rangle_{\boldsymbol{k}})\sin^2\delta_0} \qquad (3)$$

and $\delta_0 = \tan^{-1}(\pi N_0 u_0)$ with impurity strength u_0. N_0 is the DOS at the Fermi energy in the normal state. In the Born limit of weak impurity scattering potential, $\delta_0 \to 0$. In the unitary limit of strong scattering potential, $\delta_0 \to \pi/2$. The scattering time τ_0 in the normal state is given by $1/\tau_0 = n_s N_0 u_0^2/(1 + \pi^2 N_0^2 u_0^2)$, where n_s is the number density of impurities. τ_0 is in unit of $2\pi k_\mathrm{B}T_\mathrm{c}/\hbar$ [23].

As for self-consistent conditions, the pair potential is calculated by the gap equation

$$\Delta(\boldsymbol{r}) = g_0 N_0 T \sum_{0<\omega_n\leqslant\omega_\mathrm{cut}} \langle\varphi_d^*(f + f^{\dagger *})\rangle_{\boldsymbol{k}} \qquad (4)$$

with $(g_0 N_0)^{-1} = \ln T + 2T\sum_{0<\omega_n\leqslant\omega_\mathrm{cut}}\omega_n^{-1}$. We use $\omega_\mathrm{cut} = 20 k_\mathrm{B}T_\mathrm{c}$. The vector potential for the internal magnetic field is self-consistently determined by

$$\nabla\times(\nabla\times\boldsymbol{A}) = -\frac{2T}{\kappa^2}\sum_{0<\omega_n}\langle\boldsymbol{v}\mathrm{Im}g\rangle_{\boldsymbol{k}}. \qquad (5)$$

We set the Ginzburg-Landau parameter $\kappa = 30$ assuming typical type-II superconductors.

First, we solve Eqs. (1)–(5) at $T = 0.5T_c$, and obtain self-consistent solutions of $\Delta(\boldsymbol{r})$, $\boldsymbol{A}(\boldsymbol{r})$, and quasiclassical Green's functions [33]. We perform the calculations for $1/\tau_0 = 0.01$, 0.05, and 0.1 in the Born and the unitary limits, in addition to the clean limit $1/\tau_0 = 0$.

Next, we study local electronic states, assuming that the T dependences of $\Delta(\boldsymbol{r})$ and $\boldsymbol{A}(\boldsymbol{r})$ at low temperature $T \leqslant 0.5T_c$ do not seriously change the results. Thus, using the self-consistently obtained $\Delta(\boldsymbol{r})$ and $\boldsymbol{A}(\boldsymbol{r})$ in the calculation of ω_n, we solve Eqs. (1)–(3) with $i\omega_n \to E + i\eta$ to obtain $g(i\omega_n \to E + i\eta, \boldsymbol{k}, \boldsymbol{r})$ as a function of real energy E. η is an infinitesimal constant. The local DOS, which is proportional to low temperature specific heat, is obtained by

$$N(E, \boldsymbol{r}) = \int_0^{2\pi} \frac{d\theta}{2\pi} N(E, \theta, \boldsymbol{r}) = \int_0^{2\pi} \frac{d\theta}{2\pi} \int_0^{2\pi} \frac{dk_c}{2\pi} N(\boldsymbol{k}) g(i\omega_n \to E + i\eta, \boldsymbol{k}, \boldsymbol{r}), \tag{6}$$

where $N(\boldsymbol{k})$ is the $\mathbf{k}$-resolved DOS on the Fermi surface, and $N_0 = \int_0^{2\pi} d\theta \int_0^{2\pi} dk_c N(\boldsymbol{k})/(2\pi)^2$. The zero-energy local DOS $N(E = 0, \boldsymbol{r})$ has a peak at the vortex center, as shown in Fig. 1. The peak structure is smeared with increasing $1/\tau_0$, and the smearing effect is greater in the unitary limit than in the Born limit. The DOS $N(E)$ and the θ-resolved DOS $N(E, \theta)$ are, respectively, spatial average of $N(E, \boldsymbol{r})$ and $N(E, \theta, \boldsymbol{r})$ as

$$N(E) = \langle N(E, \boldsymbol{r}) \rangle_{\boldsymbol{r}}, \quad N(E, \theta) = \langle N(E, \theta, \boldsymbol{r}) \rangle_{\boldsymbol{r}}. \tag{7}$$

We study B dependence of the vortex states for several values of $1/\tau_0$ comparatively in the Born and the unitary limits. Figure 2 presents the spatially-averaged amplitude of the pair potential, $\langle |\Delta(\boldsymbol{r})| \rangle_{\boldsymbol{r}}$, as a function of B. The amplitude decreases with increasing B and vanishes at the upper critical field H_{c2}. With increasing $1/\tau_0$, the amplitude and H_{c2} become smaller, since the d-wave superconductivity is suppressed by the nonmagnetic impurity scattering. When we compare two cases of the field orientations; $\phi = 0^\circ$ ($\boldsymbol{B} \parallel$ antinode) and $\phi = 45^\circ$ ($\boldsymbol{B} \parallel$ node), H_{c2} is larger for $\phi = 0^\circ$. As for the difference between (a) the Born limit and (b) the unitary limit, $\langle |\Delta(\boldsymbol{r})| \rangle_{\boldsymbol{r}}$ is slightly smaller in the unitary limit at low B. H_{c2} is the same for the two limits, because $1/\tau$ in Eq. (3) becomes the same when $g \to 1$, $f \to 0$, $f^\dagger \to 0$ at $B = H_{c2}$.

In Fig. 3, we present B dependence of zero-energy DOS $N(E = 0)$, which corresponds to the low temperature specific heat. In the Born limit in Fig. 3(a), with increasing $1/\tau_0$ $N(E = 0)$ becomes larger, reflecting the suppression of H_{c2} by the impurity scattering. In the unitary limit in Fig. 3(b), with increasing $1/\tau_0$ $N(E = 0)$ increases even at a zero field $B = 0$ in addition to the suppression of H_{c2} [34,35]. In Fig. 3, solid lines present $N_{\rm antinode} \equiv N(E = 0)|_{\phi=0^\circ}$ for the field orientation $\boldsymbol{B} \parallel$ antinode. Dashed lines present $N_{\rm node} \equiv N(E = 0)|_{\phi=45^\circ}$ for $\boldsymbol{B} \parallel$ node. In all cases of Fig. 3, $N_{\rm antinode} < N_{\rm node}$ at higher B, since H_{c2} is smaller for $\boldsymbol{B} \parallel$ node.

To discuss the oscillation of $N(E = 0)$ under the rotation of in-plane magnetic field, in Fig. 4(a) we present the field orientation ϕ dependence of $N(E = 0)/\bar{N}$ at $B = 0.2$ with $\bar{N} = (N_{\rm antinode} + N_{\rm node})/2$. In the clean limit, as in previous studies [11,13,14], $N(E = 0)$ has minimum at $\phi = 45^\circ$, i.e., $N_{\rm antinode} > N_{\rm node}$. However in the presence of impurity scattering with $1/\tau_0 = 0.1$ in both the Born and the unitary limits, the sign of oscillation is changed, so that $N_{\rm antinode} < N_{\rm node}$, i.e., $N(E = 0)$ has minimum at $\phi = 0^\circ$. To discuss B dependence of the oscillation, we present $dN \equiv (N_{\rm antinode} - N_{\rm node})/\bar{N}$ as a function of B in Fig. 4(b). In the clean limit, $dN > 0$ at low B, while $dN < 0$ at high B, as is observed in a $d_{x^2-y^2}$-wave superconductor $CeCoIn_5$ [2,3].

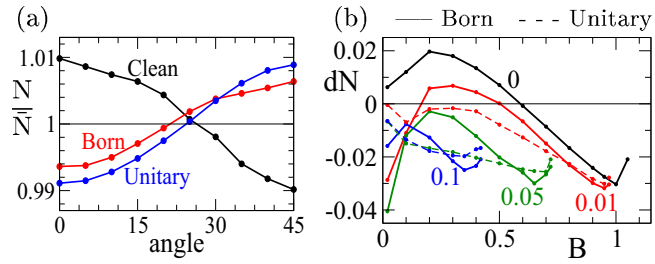

FIG. 4. (a) Normalized zero-energy DOS $N(E = 0)/\bar{N}$ as a function of field orientation angle ϕ for $1/\tau_0 = 0.1$ in the Born and the unitary limits in addition to the clean limit. $B = 0.2$. (b) $dN \equiv (N_{\rm antinode} - N_{\rm node})/\bar{N}$ as a function of B for $1/\tau_0 = 0$, 0.01, 0.05, and 0.1. Solid (dashed) lines are for the Born limit (the unitary limit).

However, when the strength of the impurity scattering increases, dN becomes negative even at low B in both the Born and the unitary limits. We expect that future measurements will detect these impurity effects in the B dependence, which may give significant contributions on the angle-resolved specific heat. Since a fundamental case of $d_{x^2-y^2}$-wave pairing is considered in the present work, calculations for complicated s_{+-} or s_{++} wave pairings on multibands, such as in Fe-based superconductors, belong to future studies. In this work, we studied zero-energy DOS proportional to low temperature specific heat. It is worth mentioning that the sign of the oscillation may be reversed even in a clean superconductor on raising T [3,15–17]. The sign change by T reflects the field orientation dependence of DOS spectrum $N(E)$ at finite E [16,17]. The T dependence of the angle-resolved specific heat belongs to future studies because we have to perform further heavier calculation about the T dependence of the free energy [15] or the E dependence of the DOS [16,17] in the various cases of the impurity scatterings.

Lastly, we study the θ-resolved DOS $N(E = 0, \theta)$, which is often used to explain the difference between $N_{\rm antinode}$ and $N_{\rm node}$. As shown in Fig. 5, $N(E = 0, \theta)$ is distributed around nodes of $\varphi_d(\theta)$ on the Fermi surface. In the evaluation of the Doppler shift by the phase winding around a vortex [11,12], $N(E = 0, \theta)$ equally appears at four nodes when $\boldsymbol{B} \parallel$ antinode, as schematically shown in Fig. 5(a). When $\boldsymbol{B} \parallel$ node in Fig. 5(b), it largely appears at two nodes with $\boldsymbol{k} \perp \boldsymbol{B}$ but remains small at other two nodes with $\boldsymbol{k} \parallel \boldsymbol{B}$. While these distributions are used to explain the result $N_{\rm antinode} > N_{\rm node}$ in the clean limit at low B, we need to quantitatively consider $N(E = 0, \theta)$ in Figs. 5(c) and 5(d), which include vortex core contributions by self-consistent Eilenberger theory

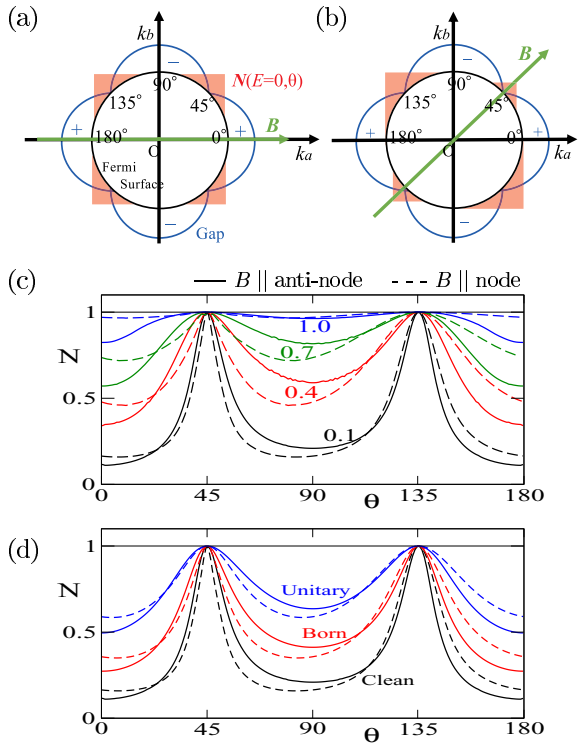

FIG. 5. (a) Relation of $d_{x^2-y^2}$ wave gap $|\varphi_d(\theta)|$ and zero-energy DOS $N(E=0,\theta)$ is schematically presented on the circular Fermi surface for $\boldsymbol{B} \parallel$ antinode of $\phi = 0°$. (b) The same as (a), but for $\boldsymbol{B} \parallel$ node of $\phi = 45°$. (c) θ dependence of Fermi surface DOS $N(E=0,\theta)/N_0$ for $\boldsymbol{B} \parallel$ antinode of $\phi = 0°$ (solid lines) and for $\boldsymbol{B} \parallel$ node of $\phi = 45°$ (dashed lines) at $B = 0.1$, 0.4, 0.7, and 1.0 in the clean limit. (d) The same as (c) but at $B = 0.1$ in the Born and the unitary limits with $1/\tau_0 = 0.1$, in addition to the clean limit $1/\tau_0 = 0$.

calculations. There, $N(E=0,\theta)$ has peaks at the nodes $\theta = 45°$ and 135°. In Fig. 5(c), we see that width of the peak becomes wider with increasing B. In Fig. 5(d), the broadening by the impurity scatterings is pronounced in the unitary limit than in the Born limit.

Both in Figs. 5(c) and 5(d), peaks at $\theta = 45°$ and 135° have the same width, when $\boldsymbol{B} \parallel$ antinode presented by solid lines. On the other hand, when $\boldsymbol{B} \parallel$ node presented by dashed lines, the peak at $\theta = 135°$ of $\boldsymbol{k} \perp \boldsymbol{B}$ is wider than that at $\theta = 45°$ of $\boldsymbol{k} \parallel \boldsymbol{B}$. Compared to the clean limit at low B where $N_{\text{antinode}} > N_{\text{node}}$, difference between dashed lines ($\boldsymbol{B} \parallel$ node) and solid lines ($\boldsymbol{B} \parallel$ antinode) increases near $\theta = 0°$ for larger $1/\tau_0$ or higher B. Therefore, N_{node} is enhanced so that $N_{\text{antinode}} < N_{\text{node}}$ by impurity scattering or B. We note that the contribution of $N(E=0,\theta=0°)$ at an antinode is not negligible in Figs. 5(c) and 5(d). Thus, discussions based on simple pictures of Figs. 5(a) and 5(b) are not always valid in the presence of vortex core contributions.

In summary, based on the Eilenberger theory, we theoretically studied nonmagnetic impurity scattering effects on the oscillation of zero-energy DOS under the rotation of in-plane magnetic field in a $d_{x^2-y^2}$-wave superconductor, which can be compared to low temperature specific heat measurements. We found that the sign of the oscillation can be changed by the impurity scattering and clarified its dependence on the magnetic field B and the scattering rates $1/\tau_0$. These results suggest that the impurity scattering effects also play decisive role in the analysis of the angle-resolved specific heat to identify node positions of the pairing function in unconventional superconductivity.

This work was supported by JSPS KAKENHI Grant No. 17K05542.

[1] T. Sakakibara, A. Yamada, J. Custers, K. Yano, T. Tayama, H. Aoki, and K. Machida, Nodal structures of heavy fermion superconductors probed by the specific-heat measurements in magnetic fields, J. Phys. Soc. Jpn. **76**, 051004 (2007).

[2] T. Sakakibara, S. Kittaka, and K. Machida, Angle-resolved heat capacity of heavy fermion superconductors, Rep. Prog. Phys. **79**, 094002 (2016).

[3] K. An, T. Sakakibara, R. Settai, Y. Onuki, M. Hiragi, M. Ichioka, and K. Machida, Sign Reversal of Field-Angle Resolved Heat Capacity Oscillations in a Heavy Fermion Superconductor $CeCoIn_5$ and $d_{x^2-y^2}$ Pairing Symmetry, Phys. Rev. Lett. **104**, 037002 (2010).

[4] S. Yonezawa, K. Tajiri, S. Nakata, Y. Nagai, Z. Wang, K. Segawa, Y. Ando, and Y. Maeno, Thermodynamic evidence for nematic superconductivity in $Cu_xBi_2Se_3$, Nat. Phys. **13**, 123 (2016).

[5] K. Deguchi, Z. Q. Mao, H. Yaguchi, and Y. Maeno, Gap Structure of the Spin-Triplet Superconductor Sr_2RuO_4 Determined from the Field-Orientation Dependence of the Specific Heat, Phys. Rev. Lett. **92**, 047002 (2004).

[6] S. Kittaka, S. Nakamura, T. Sakakibara, N. Kikugawa, T. Terashima, S. Uji, D. A. Sokolov, A. P. Mackenzie, K. Irie, Y. Tsutsumi, K. Suzuki, and K. Machida, Searching for gap zeros in Sr_2RuO_4 via field-angle-dependent specific-heat measurement, J. Phys. Soc. Jpn. **87**, 093703 (2018).

[7] S. Kittaka, Y. Aoki, N. Kase, T. Sakakibara, T. Saito, H. Fukazawa, Y. Kohori, K. Kihou, C. H. Lee, A. Iyo, H. Eisaki, K. Deguchi, N. K. Sato, Y. Tsutsumi, and K. Machida, Thermodynamic study of nodal structure and multiband superconductivity of KFe_2As_2, J. Phys. Soc. Jpn. **83**, 013704 (2014).

[8] B. Zeng, G. Mu, H. Q. Luo, T. Xiang, I. I. Mazin, H. Yang, L. Shan, C. Ren, P. C. Dai, and H.-H. Wen, Anisotropic structure of the order parameter in $FeSe_{0.45}Te_{0.55}$ revealed by angle-resolved specific heat, Nat. Commun. **1**, 112 (2010).

[9] Y. Sun, S. Kittaka, S. Nakamura, T. Sakakibara, K. Irie, T. Nomoto, K. Machida, J. Chen, and T. Tamegai, Gap structure of FeSe determined by angle-resolved specific heat measurements in applied rotating magnetic field, Phys. Rev. B **96**, 220505(R) (2017).

[10] Y. Sun, S. Kittaka, S. Nakamura, T. Sakakibara, P. Zhang, S. Shin, K. Irie, T. Nomoto, K. Machida, J. Chen, and T. Tamegai, Disorder-sensitive nodelike small gap in FeSe, Phys. Rev. B **98**, 064505 (2018).

[11] I. Vekhter, P. J. Hirschfeld, J. P. Carbotte, and E. J. Nicol, Anisotropic thermodynamics of d-wave superconductors in the vortex state, Phys. Rev. B **59**, R9023 (1999).

[12] G. E. Volovik, Superconductivity with lines of GAP nodes: density of states in the vortex, Pis'ma Zh. Eksp. Teor. Fiz. **58**, 457 (1993) [JETP Lett. **58**, 469 (1993)].

[13] P. Miranović, N. Nakai, M. Ichioka, and K. Machida, Orientational field dependence of low-lying excitations in the mixed state of unconventional superconductors, Phys. Rev. B **68**, 052501 (2003).

[14] P. Miranović, M. Ichioka, K. Machida, and N. Nakai, Theory of gap-node detection by angle-resolved specific heat measurement, J. Phys.: Condens. Matter **17**, 7971 (2005).

[15] M. Hiragi, K. M. Suzuki, M. Ichioka, and K. Machida, Vortex state and field-angle resolved specific heat oscillation for $H \parallel ab$ in d-wave superconductors, J. Phys. Soc. Jpn. **79**, 094709 (2010).

[16] A. Vorontsov and I. Vekhter, Nodal Structure of Quasi-Two-Dimensional Superconductors Probed by a Magnetic Field, Phys. Rev. Lett. **96**, 237001 (2006).

[17] A. Vorontsov and I. Vekhter, Unconventional superconductors under a rotating magnetic field. I. Density of states and specific heat, Phys. Rev. B **75**, 224501 (2007).

[18] G. Eilenberger, Transformation of Gorkov's equation for type II superconductors into transport-like equations, Z. Phys. **214**, 195 (1968).

[19] U. Klein, Microscopic calculations on the vortex state of type II superconductors, J. Low Temp. Phys. **69**, 1 (1987).

[20] M. Ichioka, A. Hasegawa, and K. Machida, Vortex lattice effects on low-energy excitations in d-wave and s-wave superconductors, Phys. Rev. B **59**, 184 (1999).

[21] M. Ichioka, A. Hasegawa, and K. Machida, Field dependence of the vortex structure in d-wave and s-wave superconductors, Phys. Rev. B **59**, 8902 (1999).

[22] P. Miranović, M. Ichioka, and K. Machida, Effects of nonmagnetic scatterers on the local density of states around a vortex in s-wave superconductors, Phys. Rev. B **70**, 104510 (2004).

[23] K. K. Tanaka, M. Ichioka, N. Nakai, and K. Machida, Knight shift spectrum in vortex states in s- and d-wave superconductors on the basis of Eilenberger theory, Phys. Rev. B **89**, 174504 (2014).

[24] E. V. Thuneberg, J. Kurkijärvi, and D. Rainer, Elementary-flux-pinning potential in type-II superconductors, Phys. Rev. B **29**, 3913 (1984).

[25] Y. Kato, Phase-sensitive impurity effects in vortex core of moderately clean chiral superconductors, J. Phys. Soc. Jpn. **69**, 3378 (2000).

[26] M. Eschrig, D. Rainer, and J. A. Sauls, *Vortices in Unconventional Superconductors and Superfluids*, edited by R. P. Huebener, N. Schopohl, and G. E. Volovik (Springer, Heidelberg, 2002), p. 175; M. Eschrig, D. Rainer, and J. A. Sauls, arXiv:cond-mat/0106546.

[27] N. Hayashi and Y. Kato, Elementary vortex pinning potential in a chiral p-wave superconductor, Phys. Rev. B **66**, 132511 (2002).

[28] N. Hayashi, Y. Kato, and M. Sigrist, Impurity effect on Kramer-Pesch core shrinkage in s-wave vortex and chiral p-wave vortex, J. Low Temp. Phys. **139**, 79 (2005).

[29] J. A. Sauls and M. Eschrig, Vortices in chiral, spin-triplet superconductors and superfluids, New J. Phys. **11**, 075008 (2009).

[30] N. Schopohl and K. Maki, Quasiparticle spectrum around a vortex line in a d-wave superconductor, Phys. Rev. B **52**, 490 (1995).

[31] P. Miranović and K. Machida, Thermodynamics and magnetic field profiles in low-κ type-II superconductors, Phys. Rev. B **67**, 092506 (2003).

[32] M. Ichioka, V. G. Kogan, and J. Schmalian, Locking of length scales in two-band superconductors, Phys. Rev. B **95**, 064512 (2017).

[33] See Supplemental Material at http://link.aps.org/supplemental/10.1103/PhysRevB.101.060501 for the details of formulation and the calculation methods.

[34] P. J. Hirschfeld, P. Wölfle, and D. Einzel, Consequences of resonant impurity scattering in anisotropic superconductors: Thermal and spin relaxation properties, Phys. Rev. B **37**, 83 (1988).

[35] C. Kübert and P. J. Hirschfeld, Vortex contribution to specific heat of dirty d-wave superconductors: Breakdown of scaling, Solid State Commun. **105**, 459 (1998).